Chinese Journal of Chemistry, **2004**, *22*, 14—18

Article

Study on the Phase Equilibrium of the Ternary System Ethanol-Cesium Carbonate-Water at 10, 30 and 50 ℃

ZHAI, Quan-Guo[a](翟全国) HU, Man-Cheng*,[a](胡满成)
LIU, Zhi-Hong[a](刘志宏) XIA, Shu-Ping[b](夏树屏)

[a] *School of Chemistry and Materials Science, Shaanxi Normal University, Xi'an, Shaanxi 710062, China*
[b] *Xi'an Branch, Institute of Salt Lake, Chinese Academy of Sciences, Xi'an, Shaanxi 710043, China*

The phase diagrams of the CH_3CH_2OH-Cs_2CO_3-H_2O system were determined at 10, 30 and 50 ℃, respectively. It was found that the effect of the temperature on the phase equilibrium was insignificant within the investigated range. The binodal curves were given using a five-parameter equation and the tie lines were fitted using the Othmer-Tobias and Bancroft correlations. Correlation coefficients (R) for all equations exceeded 0.99. Samples of the solid phase at 30 ℃ were analyzed by TGA showing that it consisted of $Cs_2CO_3 \cdot 3.5H_2O$. The refractive index of the systems was also determined.

Keywords liquid-liquid equilibrium, phase diagram, Cs_2CO_3, binadol curve, tie line

Introduction

The salting out effect in the systems of aliphatic alcohol-water is of industrial interest. The addition of organic solvents to the aqueous solution of a salt normally decreases the solubility of the salt. So the method can be used for salting-out of inorganic salts to improve yield and purity.[1-3] However, the phase diagrams of the investigated systems are required as basic data. There are lots of aliphatic alcohol-water systems having been determined. The 1-butanol-water-NaCl system at 20, 25, 40 and 50 ℃ was measured by Santis *et al.*[4,5] The 1-butanol-water-KCl/KBr systems were investigated by Li *et al.*[6] Gomis *et al.*[7,8] determined the phase diagrams at 25 ℃ for 1-propanol/2-propanol-NaCl/KCl/LiCl-water systems and obtained the complete phase diagrams for the systems. Mydlarz *et al.*[9] presented the solubility and density data for aqueous solutions of K_2SO_4 with 2-propanol between 20 and 50 ℃. They found that the presence of 1-propanol significantly reduced the solubility of potassium sulfate. Zafarani-Moattar *et al.*[10,11] investigated the ethanol/1-propanol/2-propanol/2-methyl-2-propanol-Mg_2SO_4/$(NH_4)_2HPO_4$/$NH_4H_2PO_4$-H_2O systems at 25 and 35 ℃. Wang *et al.*[12] measured the 1-propanol/2-propanol-water-KF systems.

As far as we know, there is no report on the phase diagrams of ethanol-cesium carbonate-water system, which are of interest in the design of purification methods for the cesium carbonate. The solubility of the salt is very large and changes insignificantly with the temperature. So the traditional method of purification using crystallization by cooling and evaporation is not effective. Here we report the phase diagrams of the systems in detail. These results can be also used to develop thermodynamic models of aqueous two-phase systems.[13-15]

Experimental

Materials

Analytical grade ethanol (purity＞99.5%, Xi'an), analytical grade cesium carbonate (purity＞99.5%, Jiangxi) and primary standard $K_2Cr_2O_7$ were used without further purification. Double distilled water was used in all experiments.

Apparatus and procedures

A 25-cm^3 glass vessel was used to carry out the equilibrium determination. It was provided with an external jacket in which water was kept at constant temperature. The temperature was controlled within ±0.1 ℃. The binodal curves were determined by addition of small amount of ethanol to cesium carbonate solution of known concentration until turbidity appeared, indicating the formation of two liquid phases.[16] The mass fraction of CH_3CH_2OH, Cs_2CO_3 and H_2O was obtained using an analytical balance (Shanghai) with a precision of $\pm 1 \times 10^{-7}$ kg.

Because the cesium carbonate is very expensive and its solubility is large, we designed a semimicro installation with microsampling for phase equilibrium determination (Figure 1)[17].

For the determination of the tie lines, only less than 10 cm^3 samples were needed that were prepared by

* E-mail: hmch@snnu.edu.cn
Received May 12, 2003; revised July 1, 2003; accepted September 9, 2003.
Project supported by the National Natural Science Foundation of China (No. 20171032).

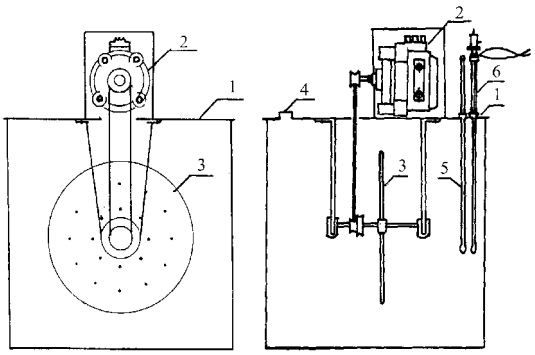

Figure 1 The semimicro installation used for phase equilibrium determination. 1—catch pan, 2—electric motor, 3—carrier plate for fixing the sample, 4—a hole to insert the heating equipment, 5—fine thermometer, 6—Beckmann thermometer.

mixing appropriate amount of ethanol, salt and water in the vessels. Samples were stirred for 48 h and then settled for 24 h to ensure that equilibrium was established. After the equilibrium was achieved, phases were withdrawn using syringes. The top phase was sampled first with care to leave a layer at least 0.5 cm thick above the interface. The bottom phase was withdrawn using a syringe with a long needle. A tiny bubble of air was retained in the needle tip and expelled once in the bottom phase to prevent contamination from upper phase material. In cases where precipitated salt was present, care was taken to ensure that sample was withdrawn without agitation, with the tip of the needle well away from salt crystals. Crystals were then filtered off and analyzed using TGA.

The concentration of the salt in the bottom phase was determined by precipitation analysis and sodium tetraphenylborate was used as precipitating agent.[18,19] The concentration of the salt in the top phase was determined using atomic absorption spectrometry (AAS). The AAS measurements were performed using a TAS-986 atomic absorption spectrometer at a wavelength of 852.1 nm. The concentration of the ethanol was determined using the oxidation process with $K_2Cr_2O_7$ as oxidant[20,21]. The reproducibility of the determination of alcohol concentration was within $\pm 0.5\%$ *W*/*W*.

The refractive index of each solution was determined using a ZAW-J refractometer with a resolution of 1×10^{-4} U and temperature was controlled within an accuracy of ± 0.1 ℃. The measurements were repeated at least three times.

Results and discussion

Binodal curve

The binodal curve data of the ethanol-cesium carbonate-water systems at 10, 30 and 50 ℃ are listed in Tables 1, 2 and 3, respectively. The binodal curves, together with the experimental tie lines are showed respectively in Figures 2, 3 and 4.

Table 1 Binodal curve data (wt%) of the CH_3CH_2OH (W_1)-Cs_2CO_3 (W_2)-H_2O (W_3) system at 10 ℃

$100W_1$	$100W_2$	$100W_1$	$100W_2$	$100W_1$	$100W_2$
85.63[a]	0.5053	59.22	5.906	4.822[b]	54.29
82.98	0.7371	45.31[a]	12.46	3.747	56.50
79.21[a]	1.005	36.49	19.09	3.035	59.61
78.13	1.097	31.59	23.00	2.483[b]	59.56
71.93	2.015	21.70	31.00	2.069	65.53
71.36[a]	2.031	11.29	42.00	1.744[b]	65.22
65.33	3.368	9.977[b]	44.80	1.298	68.02
61.96[a]	4.598	5.044	52.26	0.9600[b]	71.61

[a] Alcohol phase; [b] aqueous phase.

Table 2 Binodal curve data (wt%) of the CH_3CH_2OH (W_1)-Cs_2CO_3 (W_2)-H_2O (W_3) system at 30 ℃

$100W_1$	$100W_2$	$100W_1$	$100W_2$	$100W_1$	$100W_2$
87.38	0.7970	38.71	16.95	7.736	46.71
72.18	2.004	37.02	18.20	4.833	52.78
64.78	3.804	33.76	20.53	4.617	53.57
64.02	4.289	30.18	23.18	2.768	58.88
53.37	7.854	20.97	30.65	2.361	63.65
52.18	8.566	15.25	35.88	1.129	70.24
43.73	13.50	13.68	38.87	0.6820	73.90
43.05	14.02	12.44	39.62		
42.20	14.10	8.068	45.87		

Table 3 Binodal curve data (wt%) of the CH_3CH_2OH (W_1)-Cs_2CO_3 (W_2)-H_2O (W_3) system at 50 ℃

$100W_1$	$100W_2$	$100W_1$	$100W_2$	$100W_1$	$100W_2$
88.96	0.7700	24.74	24.18	1.637	65.00
86.12	0.7751	17.85	29.60	1.462	66.30
82.29	1.097	11.36	36.41	1.454	55.43
80.63	1.219	8.756	40.21	1.420	58.37
75.07	2.050	7.680	43.62	0.9439	71.81
72.45	2.139	5.150	47.34	0.5700	75.89
56.21	6.230	3.638	58.49		
35.73	17.23	2.740	53.17		

The binodal curves were given using the following nonlinear expression:

$$\ln W_1 = a + bW_2^{0.5} + cW_2 + dW_2^2 + eW_2^3 \quad (1)$$

where W_1 and W_2 represent the mass fraction of CH_3CH_2OH and Cs_2CO_3, respectively. The coefficient of Eq. (1) along with the corresponding standard deviations for the investigated systems are given in Table 4. On the basis of obtained standard deviations, we conclude that Eq. (1) can be satisfactorily used to correlate the binodal

curves of the investigated systems. The figures of the binodal curves can show the reliability of the model.

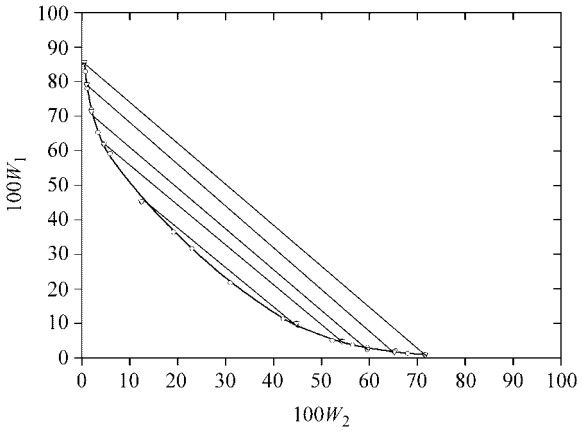

Figure 2 The binodal curve and tie lines of the CH_3CH_2OH-Cs_2CO_3-H_2O system at 10 ℃. (○) experimental data of binadol curve, (—) calculated from Eq. (1) , (△) tie lines.

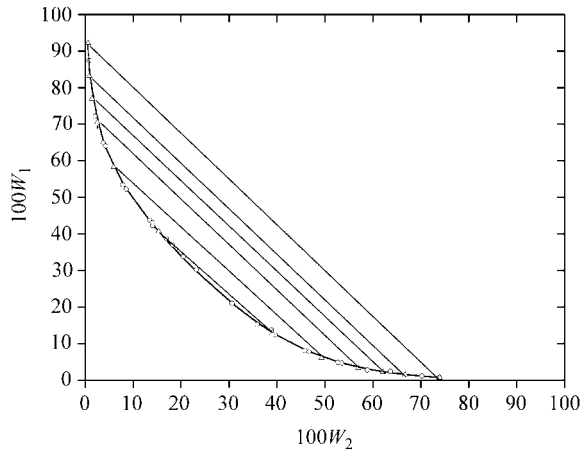

Figure 3 The binodal curve and tie lines of the CH_3CH_2OH-Cs_2CO_3-H_2O system at 30 ℃. (○) experimental data of binadol curve, (—) calculated from Eq. (1), (△) tie lines.

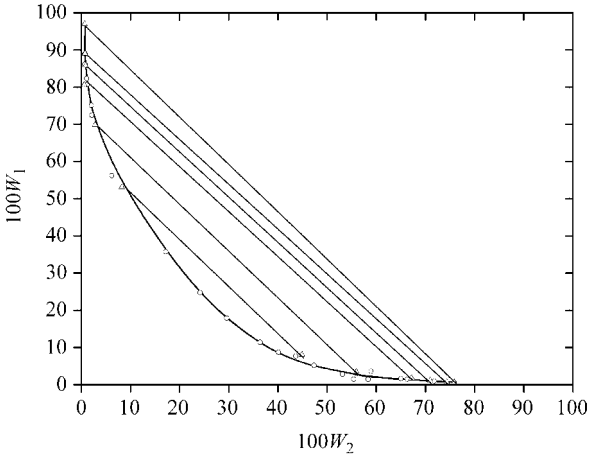

Figure 4 The binodal curve and tie lines of the CH_3CH_2OH-Cs_2CO_3-H_2O system at 50 ℃. (○) experimental data of binadol curve, (—) calculated from Eq. (1), (△) tie lines.

Table 4 Values of parameters of Eq. (1)

t/℃	a	b	c	d	e	sd[a]
10	0.077	−3.520	4.719	−12.720	3.850	0.438
30	0.127	−3.521	3.877	−10.597	2.287	0.649
50	0.174	−4.121	6.109	−20.660	13.058	0.848

[a] $sd=\sum[(100W_1^{cal}-100W_1^{exp})^2/N]^{0.5}$ where N is the number of binodal data.

Tie line

The compositions of tie lines are given in Tables 5, 6 and 7 for each temperature. In these tables, the index of refractive is high in the bottom phase because of the influence of the high salt concentration. The same result was obtained at all investigated temperatures.

Table 5 Tie line data (wt%) of the CH_3CH_2OH (W_1)-Cs_2CO_3 (W_2)-H_2O (W_3) system and refractive index n_D of the equilibrium phase at 10 ℃

Top phase			Bottom phase		
$100W_1$	$100W_2$	n_D	$100W_1$	$100W_2$	n_D
45.31	12.46	1.3715	9.977	44.80	1.3924
61.69	4.598	1.3697	4.822	54.29	1.4028
71.36	2.031	1.3696	2.483	59.56	1.4126
79.21	1.005	1.3688	1.744	65.22	1.4215
85.63[a]	0.5053	1.3680	0.9600	71.61	1.4346

[a] Solid Cs_2CO_3 present.

Table 6 Tie line data (wt %) of the CH_3CH_2OH (W_1)-Cs_2CO_3 (W_2)-H_2O (W_3) system and refractive index n_D of the equilibrium phase at 30 ℃

Top phase			Bottom phase		
$100W_1$	$100W_2$	n_D	$100W_1$	$100W_2$	n_D
40.70	15.35	1.3663	12.90	39.01	1.3814
58.26	5.920	1.3635	6.087	49.29	1.3931
70.47	2.536	1.3615	3.280	56.94	1.4046
76.92	1.416	1.3599	2.193	62.14	1.4127
83.26	0.8910	1.3607	1.444	66.73	1.42354
92.20[a]	0.5730		0.682	73.90	

[a] Solid Cs_2CO_3 present.

The reliability of the measured tie line compositions was ascertained by correlation equations given by Othmer-Tobias [Eq. (2)] and Bancroft [Eq. (3)].[16]

$$[(1-W_1^t)/W_1^t]=k_1[(1-W_2^b)/W_2^b]^n \quad (2)$$

$$(W_3^b/W_2^b)=k_2(W_3^t/W_1^t)^r \quad (3)$$

where W_1^t is the mass fraction of ethanol in the top phase, W_2^b is the mass fraction of Cs_2CO_3 in the bottom phase, W_3^b and W_3^t are respectively the mass fraction of water in the bottom and top phases. And k_1, k_2, n and r

represent fit parameters. The values of the parameter are given in Table 8. The linear dependencies of $\log[(1-W_1^t)/W_1^t]$ on $\log[(1-W_2^b)/W_2^b]$, and $\log(W_3^b/W_2^b)$ on $\log(W_3^t/W_1^t)$ indicate an acceptable consistency of the results. The corresponding correlation coefficient values, *R*, are also given in Table 8.

Table 7 Tie line data (wt%) of the CH_3CH_2OH (W_1)-Cs_2CO_3 (W_2)-H_2O(W_3) system and refractive index n_D of the equilibrium phase at 50 ℃

Top phase			Bottom phase		
$100W_1$	$100W_2$	n_D	$100W_1$	$100W_2$	n_D
53.08	8.241	1.3570	8.036	44.90	1.3851
69.84	2.814	1.3559	3.506	55.97	1.4006
80.61	0.6200	1.3546	1.760	67.20	1.4323
85.82	0.8653	1.3539	1.082	70.97	1.4302
88.96	0.7700	1.6240	0.6900	74.39	1.4568
96.92[a]	0.6880	1.6304	0.5700	75.89	1.4593

[a] Solid Cs_2CO_3 present.

Table 8 Values of parameters of Eqs. (2) and (3)

t/℃	K_1	*n*	K_2	*r*	R_1	R_2
10	1.117	0.567	0.894	1.826	0.999	0.998
30	1.251	0.582	0.740	1.805	0.999	0.999
50	1.329	0.659	0.679	1.562	0.997	0.994

Phase diagrams for CH_3CH_2OH-Cs_2CO_3-H_2O at 10, 30 and 50 ℃

Figure 5 shows the complete phase diagram of the system at 30 ℃. The letters L and S denote the liquid phase and the solid phase, respectively. Six zones are observed in the diagram. Region L represents the homogeneous zone of unsaturated liquid. In the region 2L, two liquid phases are in equilibrium: a top phase rich in ethanol, and a bottom phase rich in Cs_2CO_3. Two L+S regions are observed, where the solid phase is $Cs_2CO_3 \cdot 3.5H_2O$, but the difference is that the right represents a saturated liquid with low ethanol concentration. The saturation curve of this one begins at the solubility point of the salt in water, to the eutectic point of the aqueous phase F_I. The saturation curve of the zone to the left has a high alcohol concentration and this curve initiates in the solubility point of the salt in alcohol (A), and terminates at the vertex of pure ethanol. Both eutectics are given in Tables 5, 6 and 7 for each temperature. Two liquid and one solid phases exist in the 2L+S region. In the region L+2S, the presence of two solid phases is observed, one is $Cs_2CO_3 \cdot 3.5H_2O$ and the other is Cs_2CO_3.

The similar behavior has been found in the systems of Li_2SO_4-1-propanol-H_2O,[22] Na_2SO_4-PEG 3350-H_2O[23] and NaCl-PPG 425-H_2O.[24] However, there is a difference between the studied system and the last two: the two systems both have one kind of solid, anhydrous salt, so they have five zones.

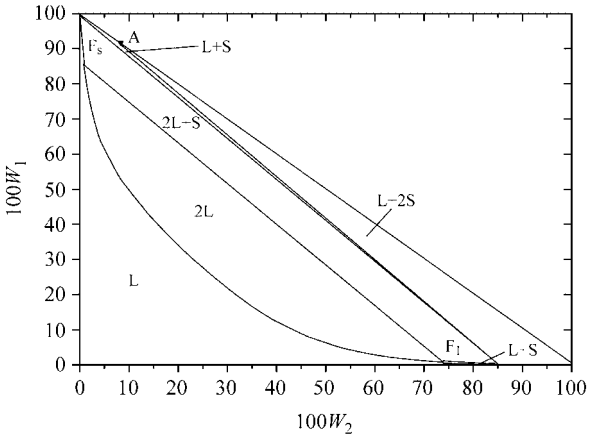

Figure 5 Phase diagram of the CH_3CH_2OH-Cs_2CO_3-H_2O system at 30 ℃. A: the solubility point of the salt in the ethanol, F_s and F_I: two eutectics.

Conclusion

For CH_3CH_2OH-Cs_2CO_3-H_2O system, binodal curves and tie lines have been determined at 10, 30 and 50 ℃, respectively. And tie line data of these systems could be satisfactorily described by Othmer-Tobias and Bancroft equations. The data obained are of interest in the design of processes for the crystallization of Cs_2CO_3.

References

1 Thompson, A. R.; Molstad, M. C. *Ind. Eng. Chem.* **1945**, *37*, 1244.
2 Hoppe, H. *Chem. Process Eng.* **1968**, *49*, 61.
3 Chen, X. J.; Li, Z. B.; Hu, R. Z. *Thermochim. Acta* **1995**, *260*, 243.
4 Santis, R. D.; Marrelli, L.; Muscetta, P. N. *J. Chem. Eng. Data* **1976**, *11*, 207.
5 Santis, R. D.; Marrelli, L.; Muscetta, P. N. *J. Chem. Eng. Data* **1976**, *21*, 324.
6 Li, Z. G.; Tang, Y. P.; Liu, Y. *Fluid Phase Equilib.* **1995**, *103*, 143.
7 Gomis, V.; Ruiz, F.; de Vera, G.; Lopez, E.; Saquete, M. D. *Fluid Phase Equilib.* **1994**, *98*, 141.
8 Gomis, V.; Ruiz, F.; Asensi, J. C.; Cayvela, P. *Fluid Phase Equilib.* **1996**, *119*, 191.
9 Mydlarz, J.; Jones, A.; Millan, A. *J. Chem. Eng. Data* **1989**, *34*, 124.
10 Zafarani-Moattar, M. T.; Salabat, A. *J. Chem. Eng. Data* **1997**, *42*, 1241.
11 Zafarani-Moattar, M. T.; Gasemi, J. *J. Chem. Eng. Data* **2002**, *47*, 525.
12 Wang, J. G.; Zhang, Y. M.; Wang, Y. R. *J. Chem. Eng. Data* **2002**, *47*, 110.
13 Haynes, C. A.; Beynon, R. A.; King, R. S.; Blanch, H. W.; Prausnitz, J. M. *J. Phys. Chem.* **1989**, *93*, 5612.
14 Kang, C. H.; Sandler, S. I. *Biotechnol. Bioeng.* **1988**, *32*, 1158.

15 Cheluget, E. L.; Marx, S.; Weber, M. E.; Vera, J. H. *J. Solution Chem.* **1994**, *23*, 275.
16 González-Tello, P. G.; Camacho, F.; Blazquez, G.; Alarcón, F. J. *J. Chem. Eng. Data* **1996**, *41*, 1333.
17 Yue, T.; Gao, S. Y.; Xia, S. P. *Rare Metals* **2000**, *24*, 238 (in Chinese).
18 Geilman, W.; Gebauhr, W. Z. *Anal. Chem.* **1953**, *139*, 161.
19 Yue, T.; Gao, S. Y.; Xia, S. P. *J. Salt Lake Sci.* **2000**, (8), 1.
20 Barahard, J. A.; Karayanmls, N. *Anal. Chem. Acta* **1962**, *26*, 253.
21 Xia, S. P.; Wang, G. F. *J. Salt Lake Sci.* **1987**, (1), 14.
22 Taboada, M. E. *Fluid Phase Equilib.* **2003**, *204*, 155.
23 Ho-Gutierrez, I.; Cheluget, E. L.; Vera, J. H.; Weber, M. E. *J. Chem. Eng. Data* **1994**, *39*, 245.
24 Cheluget, E. L.; Gelinas, S.; Vera, J. H.; Weber, M. E. *J. Chem. Eng. Data* **1994**, *39*, 127.

(E0305125 PAN, B. F.)